Penetration of unconventional spudcan foundations using back analyses of large deformation CPT profiles

Tolooiyan, Ali; Gavin, Kenneth; Dyson, Ashley P.

Important note
To cite this publication, please use the final published version (if applicable).
Please check the document version above.

Research paper

Penetration of unconventional spudcan foundations using back analyses of large deformation CPT profiles

Ali Tolooiyan [a,*], Kenneth Gavin [b], Ashley P. Dyson [a]

[a] *Computational Engineering for Sustainability Lab (CES-Lab), School of Engineering, University of Tasmania, Hobart, 7005, Australia*
[b] *Faculty of Civil Engineering and Geosciences, TU Delft, 2628 CN, Delft, Netherlands*

ABSTRACT

Accurate determination of the load-penetration behaviour of spudcan footings is vital in predicting the performance of offshore structures. Often, insufficient site investigation data is a limiting factor in assessing spudcan penetration, with the selection of suitable parameters typically derived from triaxial tests or Cone Penetrometer Test (CPT) data. A method is presented for simulating spudcan insertion in loose to medium-dense sand, based on minimal data, whereby the CPT tip resistance is used in combination with known correlations of soil properties, allowing for back analysis of CPT profiles through Large Deformation Finite Element (LDFE) simulation. The use of LDFE allows for failure mechanisms to be determined a priori, as a result of the simulation process, while a range of constitutive models can be implemented as necessary. Friction angle, dilation angle and relative density correlations are combined with a calibration of the elastic modulus, used to develop numerical models based on a set of soil sub-layers, each 1 m in depth. The resulting soil characterisations were used to calculate the load-penetration behaviour of several spudcan geometries (which deviate from conventional spudcan shapes) using the LDFE, to assess their performance. Results generated using the proposed technique show strong agreement with a presented field observations.

1. Introduction

The installation of offshore jack-up foundations typically requires the penetration of footings known as spudcans, through a process in which the structure is lowered until contact is made with the seabed, with further jacking resulting in penetration of the spudcan into the soil. Jack-up platform footings penetrate the soil until the foundation resistance is equal to the self-weight of the platform and the preload supplied in the form of ballast. Guidelines for determining the bearing capacity of spudcans in sands, such as SNAME (2002) and ISO (2012), are derived based on conventional bearing capacity formulae for shallow circular flat footings, with empirical correlation factors applied to account for the differences between traditional footings and spudcan geometries. These methods are prone to inaccuracies when selecting an appropriate angle of shearing resistance, further to limitations in conventional bearing capacity theory concerning dilatancy and compaction (Edwards et al., 2013).

Accurate predictions of load-penetration curves play a vital role in determining associated attributes, including stiffness, sliding resistance and even spudcan scour, impacting the stability and ongoing structural

reliability (Bienen et al., 2011). Overy (2012) noted that SNAME may overpredict spudcan penetration depths in loose sandy soils, recommending the use of laboratory tests in determining appropriate friction angles. In the case of both SNAME and ISO guidelines, factors including relative density, stress level and compressibility are noted to impact the operative friction angle. However, despite this, they are not explicitly accounted for in either guideline (Osborne et al., 2009). When advanced laboratory test results are unavailable (as is commonly the case with offshore jack-up installation), to determine the operative friction angle at the suitable stress level, tabulated values are recommended as part of both SNAME and API (Mangiavacchi et al., 2005). However, their applicability may be questionable for various geometries that do not closely mirror conical footings. Although spudcans are commonly circular in plan view (with a conical underside at angles ranging from 15 to 30° and a sharp spigot), a wide range of shapes and sizes are applicable depending on the manufacturer and the use of jack-up rig. Fig. 1 exhibits various spudcan footing geometries and sizes given by Randolph and Gourvenec (2017). As the calculation of the ultimate spudcan vertical bearing capacity is dependent on factors including the spudcan geometry, soil characterisations and drainage conditions, particular care is
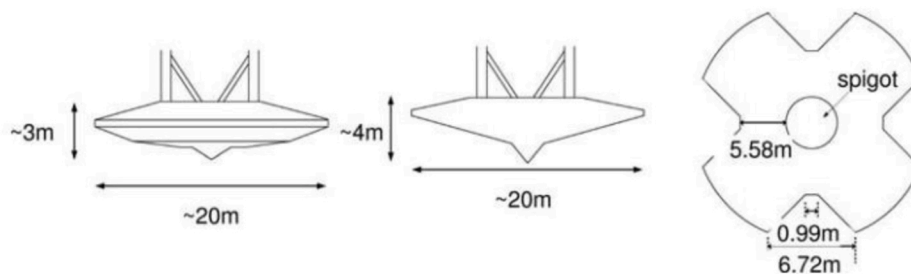

Fig. 1. Various spudcan footing dimensions and geometries (Randolph and Gourvenec, 2017).
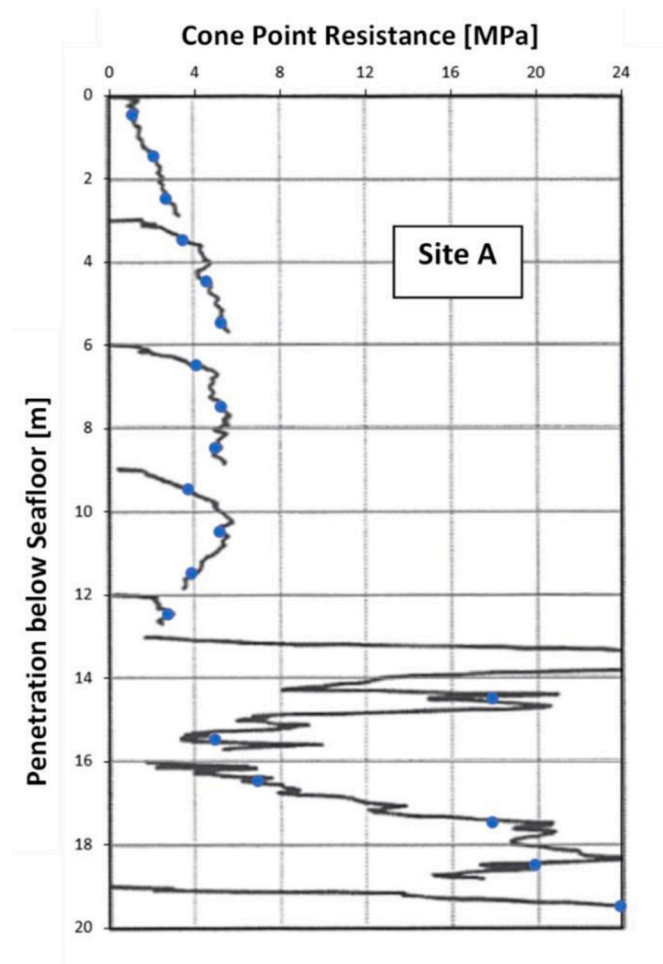

Fig. 2. CPT q_c profiles for *Site A*, after (Overy, 2012).

required for spudcan designs deviating from the conventional conical shape.

In-situ Cone Penetrometer Test (CPT) relationships can infer a range of soil parameters and are widely used for ground investigation in both onshore and offshore environments. CPTs are capable of evaluating soil properties through the measurement of the shaft (f_s) and cone end tip resistance (q_c). Published in the late 1970s, Schmertmann (1978) presented a method for predicting the settlement of shallow foundations on sand using CPT. Lunne et al. (2002) developed a set of charts providing relationships between friction angles (by way of relative density) and CPT results. More recently, Large Deformation Finite Element (LDFE) analyses have been used to investigate the continuous penetration response of spudcan foundations, cone penetration tests and pile insertions (Hossain and Randolph, 2010). These methods require no assumptions regarding the failure mechanisms and are capable of

representing appropriate soil behaviour, given the selection of a suitable constitutive soil model. In a contemporary setting, various LDFE methods exist for offshore geotechnical assessment of spudcan penetration, including (but not limited to) the Arbitrary Lagrangian Eulerian method (ALE) (Nazem et al., 2009; Tho et al., 2012; Tolooiyan and Gavin, 2011; Tolooiyan et al., 2023), the Remeshing for Interpolation Technique with Small Strain (RITSS) (Tian et al., 2014; Zhang et al., 2023) and the Material Point Method (MPM) (Ceccato et al., 2016; Martinelli and Galavi, 2021).

The Coupled Eulerian Lagrangian (CEL) method has been implemented to study offshore problems ranging from the behaviour of offshore pipelines (Dutta et al., 2012) to submarine landslides (Chen et al., 2020) and has been widely used in modelling both CPT (Gupta et al., 2016; Hamann et al., 2015; Zhang and Yi, 2018) and spudcan installation (Hu et al., 2014, 2015; Jun et al., 2018). Applications of CEL for spudcan penetration in sand over clay have been considered by Qiu and Grabe (2012) and Henke and Qiu (2010) with the hypoplastic constitutive model. The method overcomes mesh distortion by the use of both Lagrangian and Eulerian formulations whereby the material is tracked through the Eulerian mesh through the computation of the Eulerian Volume Fraction (EVF). Lagrangian elements pass through the Eulerian domain until they encounter Eulerian elements with a non-zero EVF.

This paper proposes a method using LDFE simulation with CEL in combination with several well-known, accepted soil correlations, to back-calculate CPT profiles based on limited data in an effort to determine appropriate soil parameters from CPT q_c profiles. The method provides a mechanism for simulating spudcan penetration for a range of shapes and sizes, the results of which strongly agree with observed spudcan bearing capacities. The performance of three distinct spudcan footings are presented along with their corresponding in-situ field test results for a case study involving sandy soils in the North Sea.

2. Site conditions and proposed method

A case history is selected based on a southern North Sea site (designated *Site A*), as presented by Overy (2012), with the deposit consisting of a loose to medium dense sand overlying dense to very dense sands. As part of the site investigations, continuous CPT profiles and laboratory tests (in the form of consolidated drained triaxial tests and multistage direct shear tests) were performed. CPT profiles for the top 20 m, performed in 3-m test intervals are given in Fig. 2, with the CPT point resistance (q_c) extracted at equal spacings of 1-m for analyses performed herein. As a result of laboratory particle size distribution tests performed in the upper sands, the majority of tested materials are considered to be within a narrow band comprising fine sands. A submerged unit weight (γ') of 9 kN/m^3 was observed in the upper stands, with a unit weight of 10 kN/m^3 associated with the underlying sands located at a 14-m below seafloor (bsf). As part of eight consolidated drained triaxial tests and ten shear box tests, a constant volume friction angle (φ_{cv}) of 32.6° was obtained with a standard deviation of 2.3°. An additional twenty particle size distribution tests were performed on the upper sand layers, with D$_{50}$ ranging from 0.8 to 0.11 mm. In the
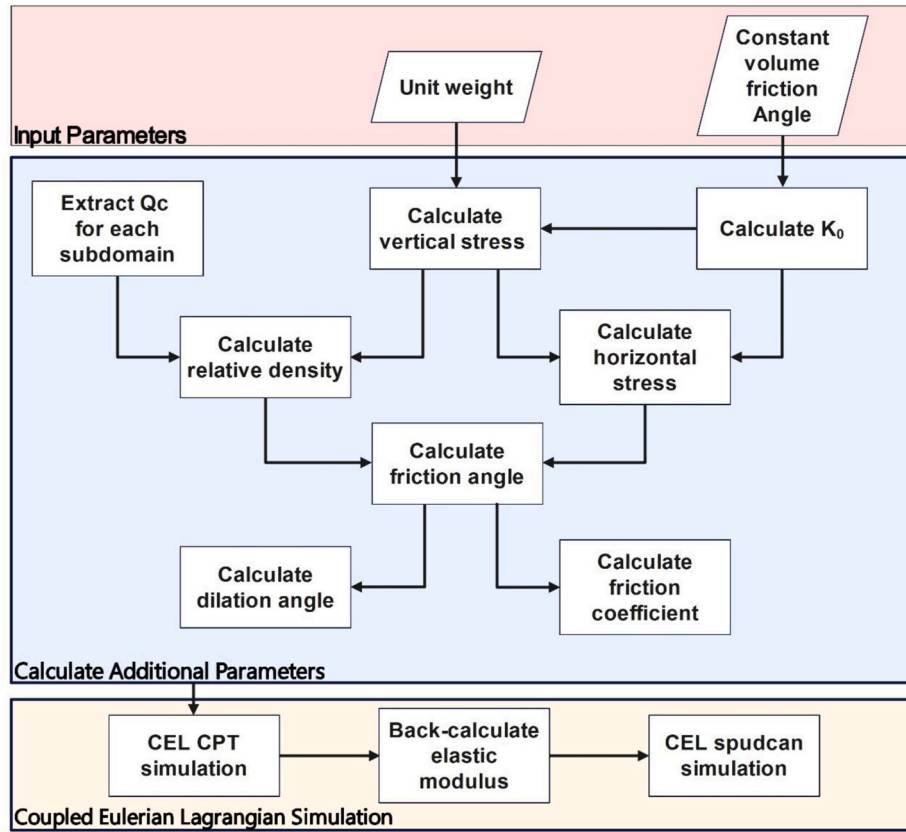
Fig. 3. Methodology describing the calculation of necessary soil parameters and the CEL simulation procedure.

simulation of spudcan penetration, the soil stiffness is back-calculated through simulation of CPT profiles. To simulate this behaviour, large deformation simulation is considered using the Coupled Eulerian Lagrangian method. Although the aforementioned soil parameters are necessary for the simulation of CPT and spudcan penetration using CEL, additional parameters are required to assess their load-penetration behaviour. The following procedure presents a method to further characterise the properties of these sands with limited site and laboratory data. Based on a series of derived relationships, back-analyses of CPT profiles are performed. With the salient soil properties of the necessary sand layers obtained, the penetration of various spudcan geometries can be considered.

Fig. 3 outlines the procedure to obtain all necessary soil parameters, thereby allowing CEL simulation of CPT and spudcan penetration to be performed. A detailed description of the assumed relationships is provided herein.

The soil domain is discretised into 20 sub-domains, each 1 m in depth. The soil properties associated with the midpoint of each sub-domain i.e., at the half-metre mark are assigned to the sub-domain of the numerical models to be presented in later sections. The CPT q_c profiles as given in Fig. 2 are extracted at 1-m increments, and the effective vertical stress (σ_v') is calculated based on the product of the unit weight and depth. Estimates of K_0 for sands have been the consideration of many studies, as summarised by Mayne and Kulhawy (1982), whereby 171 different soils were considered. For loosely deposited sands at rest, Jaly (1944) produced an analytic formulation of the coefficient for lateral earth pressure at rest (K_0), noting a decrease from unity, with a sinusoidal trend based on the effective stress friction angle (φ'):

$$K_0 = 1 - \sin \varphi' \tag{1}$$

K_0 is determined based on the constant volume friction angle and is used

to determine the horizontal stress (σ_h) for each sublayer. The relative density D_R as a function of cone resistance and vertical stress is given by Equation (2), determined by regression analyses conducted on a comprehensive set of tests performed on normally consolidated sands (Jamiolkowski et al., 1985; Lancellotta, 1983).

$$D_R = -98 + 66 \log_{10} \frac{q_c}{\sqrt{\sigma_v'}} \tag{2}$$

The peak friction angle is calculated by way of correlations measured from drained triaxial compression tests performed by Robertson and Campanella (1983), as per Equation (3) and further detailed in Fig. 4, where blue markings indicate the friction angle for *Site A* for monotonically increasing vertical effective stress values with depth. The relationship provides reasonably accurate estimates of peak friction angles for normally consolidated, uncemented sands. In cases where highly compressible sands are present, conservative results may be achieved. As an alternative, Bolton (1987) presented a procedure to consider the friction angle and dilatancy of sands through the relative dilatancy index I_{RD}:

$$I_{RD} = D_R \left(Q - \ln \frac{100}{p_a} p' \right) - 1 \tag{3}$$

where p' is the mean normal stress; p_a is the atmospheric pressure, and Q is a minerology-dependent parameter, as shown in Table 1. The difference between the peak friction angle and the critical state is determined based on the relative dilatancy index is determined by Equations (4) and (5) for triaxial and plane strain conditions, respectively (Robertson and Campanella, 1983). Two methods are presented for determining the dilatancy of loose to medium-dense sands, namely Bolton's "saw blade" relationship between the peak friction angle (φ'_{peak}), critical state friction angle (φ'_{cs}) and dilation angle (ψ) (Bolton, 1987), as shown in Equation
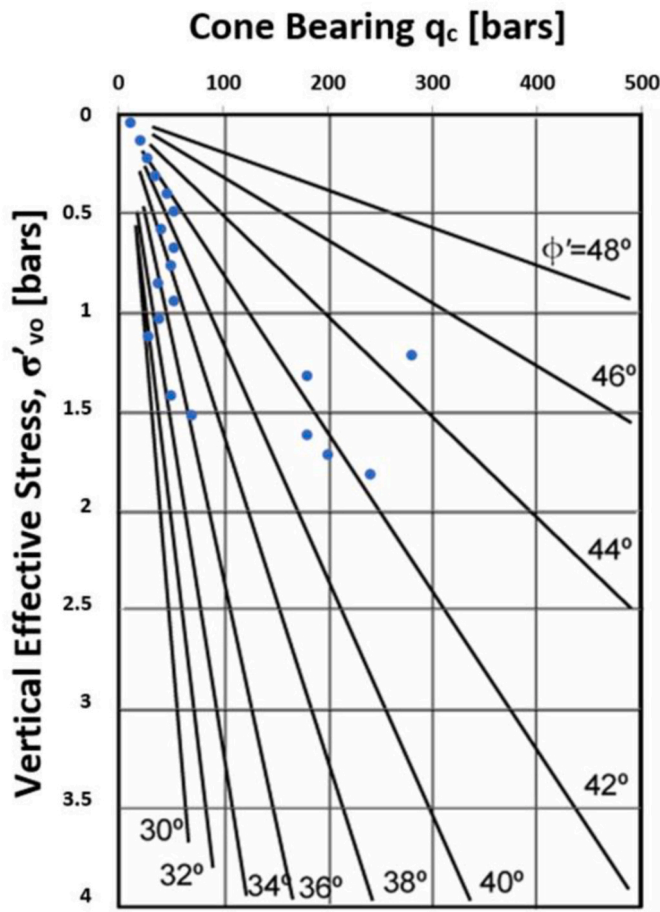
Fig. 4. Relationship between cone penetration resistance, vertical effective stress and peak friction angle for uncemented quartz sands (Robertson and Campanella, 1983).

Table 1
Mineralogy for various sands, adapted from Jamiolkowski et al. (2003).

Sand	Mineralogy	Q	φ_{cs}
Ticino	Siliceous	10.8	34.6
Toyoura	Quartz	9.8	32.0
Hokksund	Siliceous	9.2	34.0
Mol	Quartz	10.0	31.6
Ottawa	Quartz; Fines 0%	9.8	30
	Quartz; Fines 5%	10.9	32.3
	Quartz; Fines 10%	10.8	32.9
	Quartz; Fines 15%	10.0	33.1
	Quartz; Fines 20%	9.9	33.5
Antwerpian	Quartz & Glauconite	7.8–8.3	31.5
Kenya	Calcareous	9.5	40.2
Quiou	Calcareous	7.5	41.7

(6). Alternatively, Rowe's method (1971) is given by Equation (7). For the given data at *Site A*, Fig. 5 presents the depth-based friction, dilation angles and relative densities, using the Robertson and Campanella (1983), and Bolton (1987) relationships, the Rowe (1971) and Bolton (1987) relationships, and Campanella and Howie (2005) relationships respectively. As per the relative densities derived by Equation (2), the depth-based variations can be classified as ranging from loose to medium-dense sands. As is the case with the CPT profile presented in Fig. 2, the change in materials at approximately the 14m bsf where a thin dense sand lens is evident. From direct shear tests performed on a variety of materials, Durgunoglu and Mitchell (1973) recommended that an interface friction angle twice the sand peak angle of effective internal

friction be used. Accordingly, the sand-steel interface friction coefficient (μ_{ss}) between the soil and CPT cone/shaft or the spudcan is given as a simple function of the peak friction angle (Equation (8)), varying from 0.31 to 0.41 with depth (Fig. 6).

$$\varphi'_{peak} - \varphi'_{cs} = 3I_{RD} \tag{4}$$

$$\varphi'_{peak} - \varphi'_{cs} = 5I_{RD} \tag{5}$$

$$\varphi'_{peak} = \varphi'_{cs} + 0.8\psi \tag{6}$$

$$\sin \psi = \frac{\sin \varphi'_{peak} - \sin \varphi'_{cs}}{1 - \sin \varphi'_{peak} \sin \varphi'_{cs}} \tag{7}$$

$$\mu_{ss} = \tan \frac{\varphi'}{2} \tag{8}$$

Schmertmann (1970) suggested the relationship between elastic modulus and cone tip resistance

$$E_s = 2q_c \tag{9}$$

for normally consolidated (predominantly quartz) sands, with an updated version Schmertmann (1978) of

$$E_s = 2.5q_c \tag{10}$$

for equi-dimensional footings. Additional relationships between E_s and q_c are given by Holtz (1991) suggest ratios ranging from 1.5 to 4, however, Huang et al. (2004) who noted that empirical calculations tend to underestimate the role of the elastic modulus on CPT results, with respect to simulations performed using Finite Elements. The elastic modulus of each soil layer is a necessary input parameter for virtually all FE soil constitutive models, including the linear elastic perfectly plastic case detailed in this study (by way of the Drucker-Prager constitutive model). For this reason, back analyses are conducted to fulfill the necessary condition of parameters for elastic moduli with respect to depth. With the relevant input parameters obtained through a range of relationships heretofore given, back-analyses are performed by comparing simulated q_c profiles with known CPT site investigation data by way of modifying the elastic modulus until agreement is reached.

3. Back-analysis of elastic modulus with CEL cone penetration tests

Similar to the CPT field tests performed at *Site A*, a series of CPT simulations were conducted over 3-m depth intervals, resulting in a total of 7 individual CPT models. As discussed in Section 2.1, soil clusters were divided into 3 sub-layers, each 1-m thick, with the overburden stress and soil elastic modulus varied to match the results of CPT tests with observed field measurements. Exploiting the geometric symmetries of CPT simulation, axisymmetric models consisting of a 45-degree soil section (1.5 m in radius) and CPT wedge (18 mm in radius) were created for each 3-m sub-domain. Fig. 7 shows the CEL model geometry. While penetration of the cone tip was modelled, the shaft was deemed an unnecessary component of the model setup. The steel cone constituted a Lagrangian domain, using 200 10-node quadratic tetrahedral (C3D10M) elements, while the Eulerian soil domain employed 42,757 8-node Eulerian brick reduced integration (EC3D8R) elements. In-situ horizontal stresses were determined using the K_0 procedure ($K_0 = 0.46$) as described in Equation (1).

To model the constitutive behaviour of the soil domain, the non-associative Drucker-Prager (DP) model was implemented. The yield surface (Fig. 8) is considered in the $p - t$ plane with the failure and flow potential described by Equations (9) and (10), respectively:

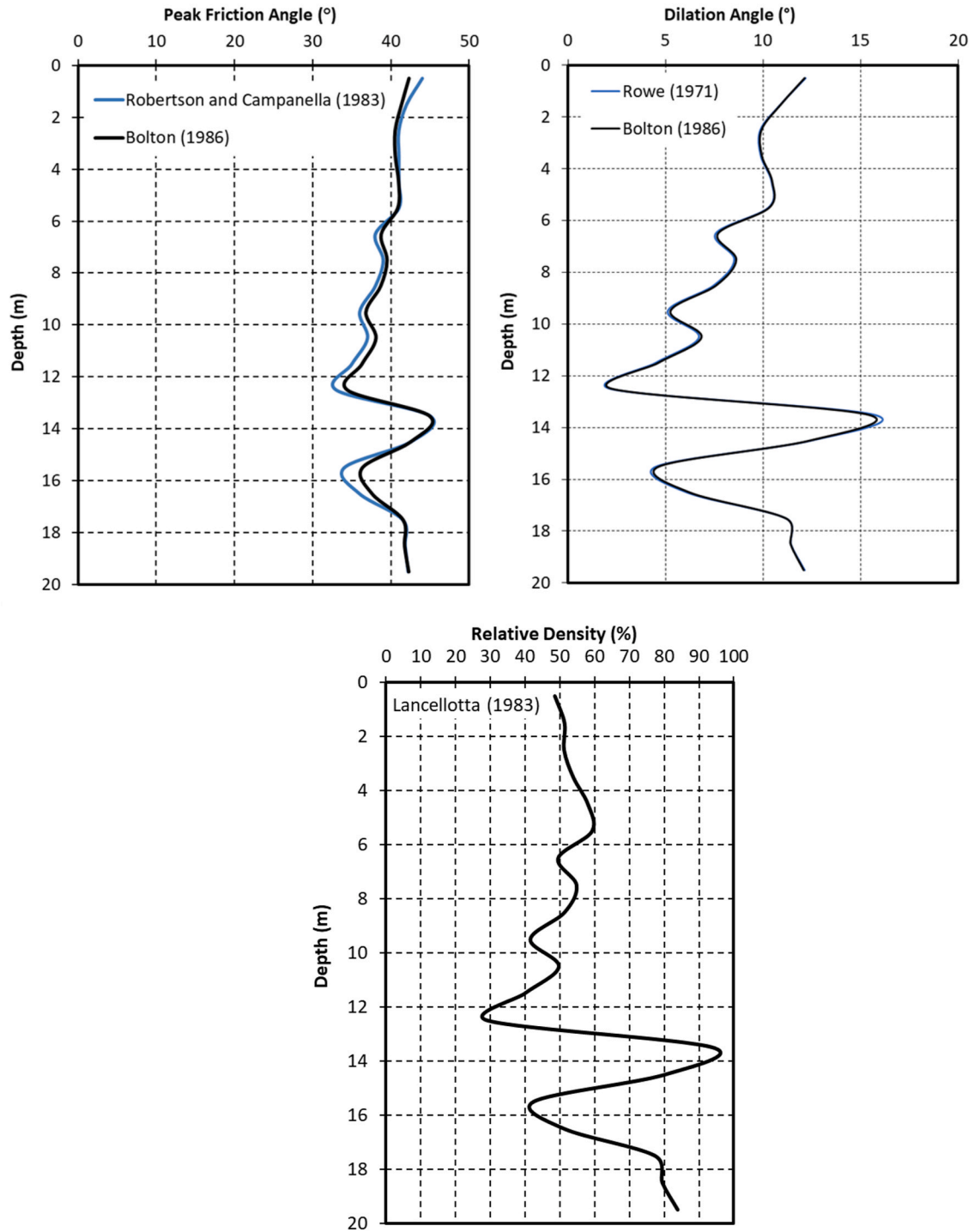$$F = t - p \tan \beta - d = 0 \tag{9}$$

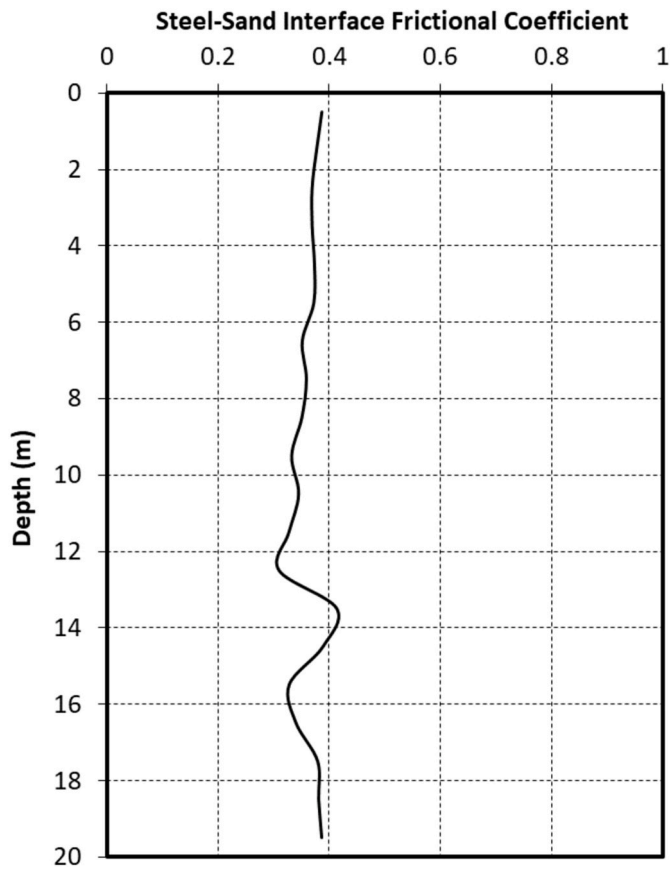**Fig. 5.** Peak friction, dilation angles and relative densities with depth for the *Site A* case study.

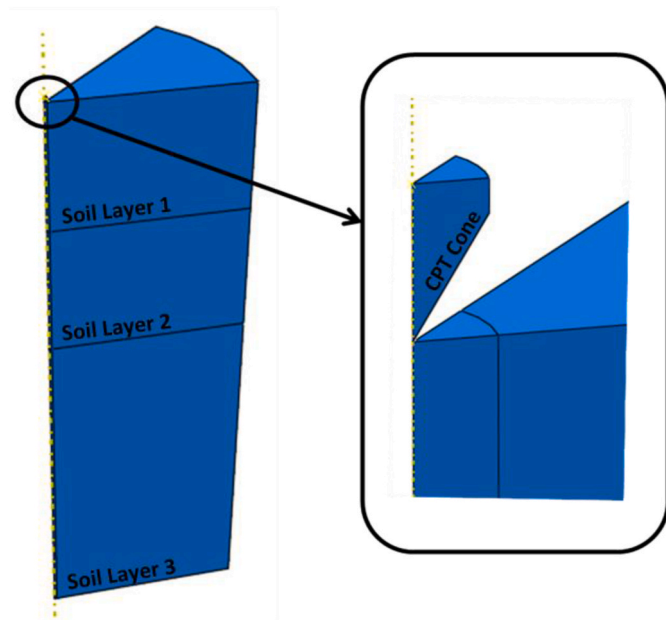**Fig. 6.** Steel-sand interface friction varying with depth.

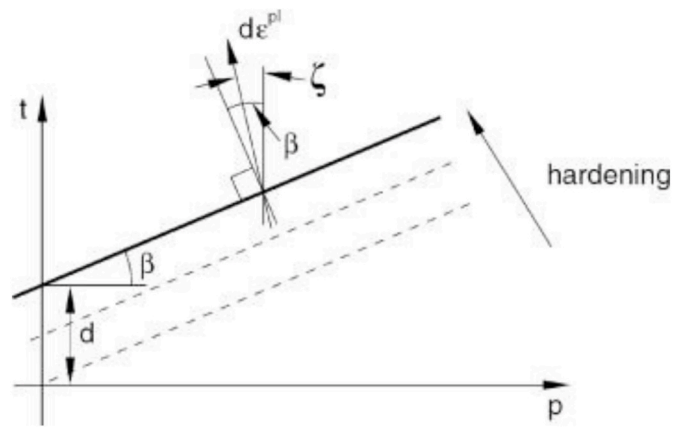**Fig. 7.** CPT axisymmetric 3-m sub-domain (45°).

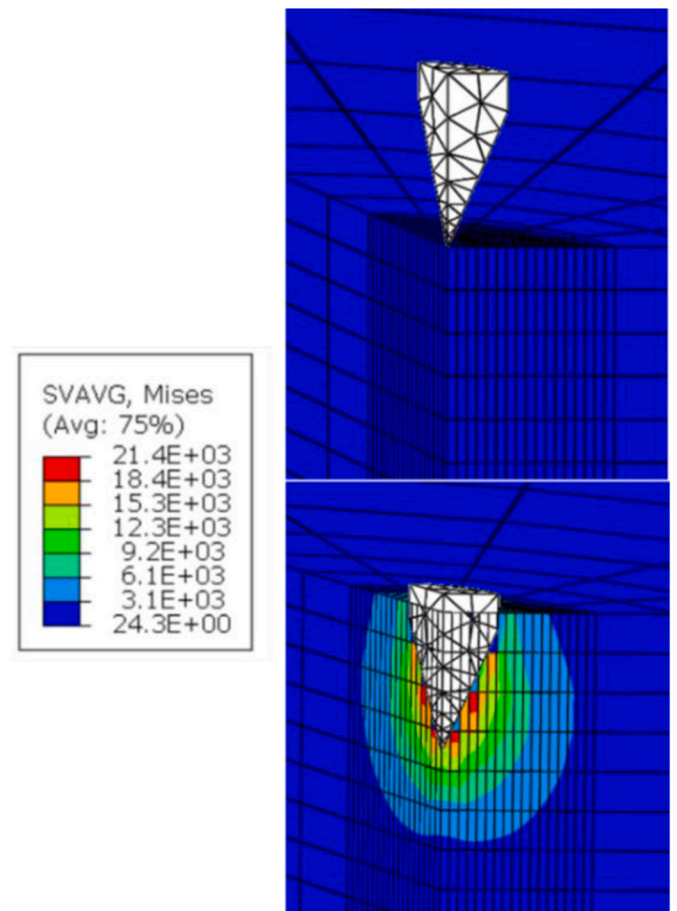**Fig. 8.** Drucker Prager yield surface and flow direction in the $p - t$ plane (Dassault Systèmes, 2022).

Fig. 9. CPT simulation mesh and stress profile.

$$p = \frac{1}{3}(\sigma_1 + 2\sigma_3) \tag{12}$$

Matching the Mohr-Coulomb failure criteria, β and d are obtained by Equations (13) and (14) (Chen and Saleeb, 2013).

$$\tan \beta = \frac{6 \sin \varphi}{3 - \sin \varphi} \tag{13}$$

$$d = c \frac{6 \sin \varphi}{3 - \sin \varphi} \tag{14}$$

As part of a two-stage analysis, simulation of an in-situ stage was

$$G = t - p \tan \zeta \tag{10}$$

where, β and d and ζ are the DP friction angle, cohesion and dilation angle, respectively. Equations 18 and 19 provide the triaxial conditions for the mean stress p and deviation stress t.

$$t = \sigma_1 - \sigma_3 \tag{11}$$
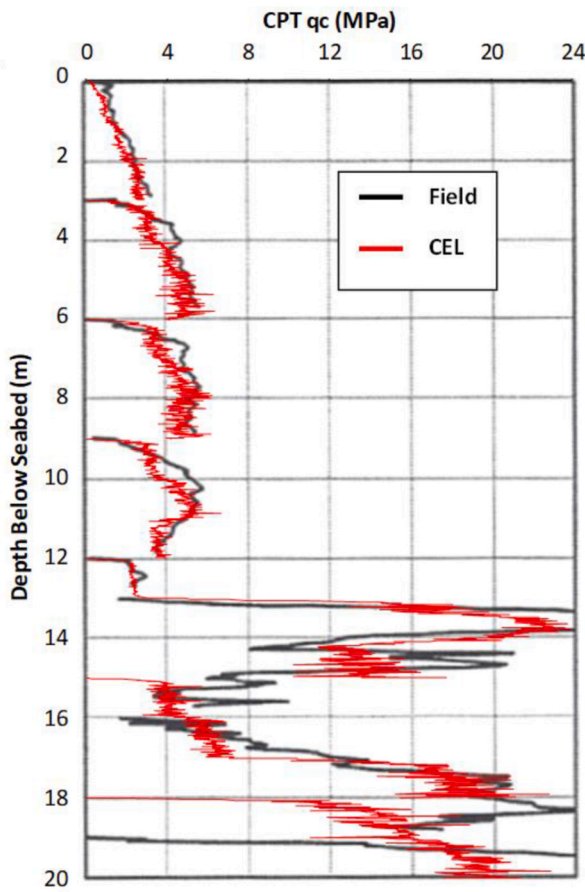
Fig. 10. Comparison of CPT q_c profile for CEL and field test results.

Fig. 11. Estimated secant stiffness profile from CEL CPT simulation.

Fig. 12. CEL simulation mesh sensitivity for CPT penetration at 18–21 m depths.

performed prior to CPT penetration. During penetration, the cone was pushed into the sand vertically at a displacement rate of 20 mm/s, as per ASTM D 5778 (2012), with the reaction force obtained at 0.1 s intervals, for a total of 150 s (i.e. 3-metre penetration) with force-displacement data also extracted. Thereafter, a sensitivity analysis was performed to ensure that the results remained unaffected by the selected penetration speed. Lagrangian contact of the cone with the Eulerian domain was considered through a tangential contact definition, with a penalty formulation applied based on the sand-steel interface friction, as a function of the peak sand friction angle. As the DP constitutive model considers a constant elastic stiffness E, the soil was discretised into sub-layer sections, each with a different elastic modulus, allowing for a back-analysis of CPT penetration. Fig. 9 provides the mesh distribution surrounding the cone tip on insertion and the stress distribution shortly thereafter. Comparison of the comparison of q_c profiles from field tests and CEL simulations is given in Fig. 10, with strong agreement observed, suitable for modelling multi-layered sandy deposits. Schmertmann (1978) considered the relationship between E_s and q_c, recommending that $E_s = 2q_c$ should be used for normally consolidated sands, while Holtz (1991) suggested E_s/q_c values of between 1.5 and 4. Combining each 3-m CPT model used to bank-analyse the elastic modulus of soil sub-layers, Fig. 11 provides the secant stiffness for the generated soil profile over the full 20-m domain, ranging from 1.25 to 2.35. Several key features of CEL-based models are necessary to ensure the validity of simulation results. One common feature of LDFE CEL cases whose mesh is not sufficiently fine is the leakage of Eulerian materials through contact surfaces and into the Lagrangian domain. As such, it is necessary to confirm that a suitably robust mesh is implemented to prohibit leakage. Eulerian penetration is most common near sharp edges and corners of Lagrangian contact surfaces. Penetration is commonly
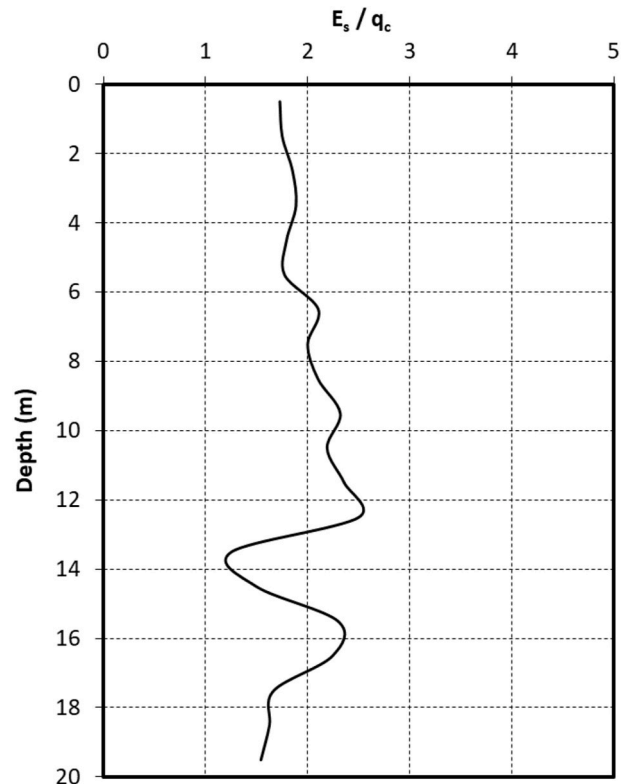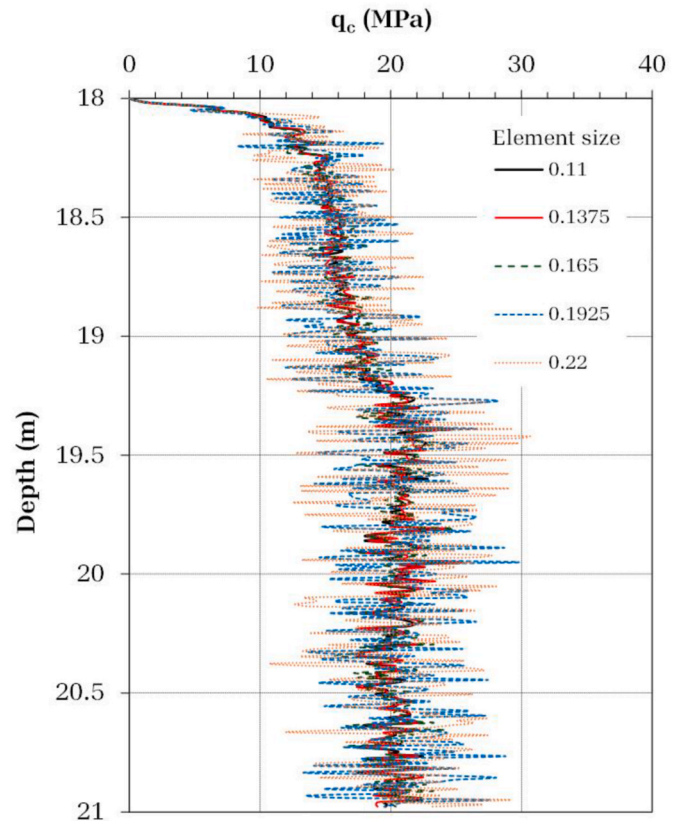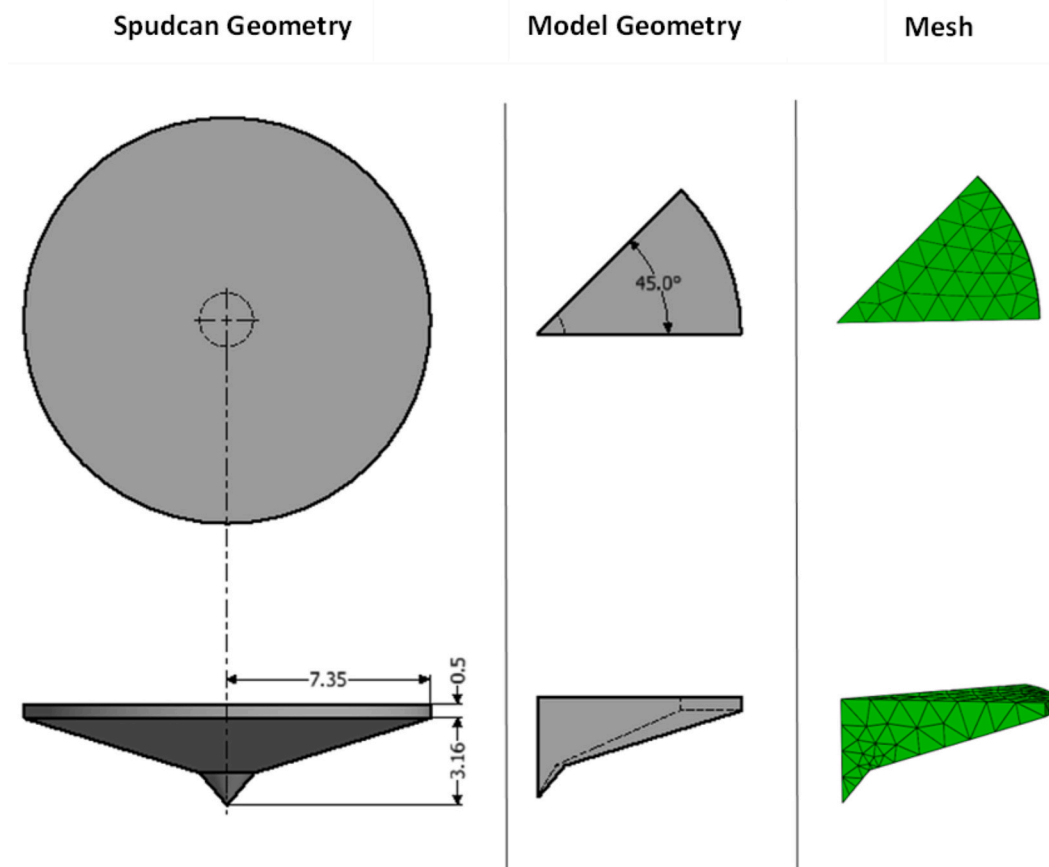
Fig. 13. MLT 116-C spudcan geometry.

minimised by refining the Eulerian mesh surrounding this zone (in this case, surrounding the CPT cone) or by filleting the Lagrangian domain to ensure that sharp edges not induce leakage. Conversely, the use of fine elements can significantly impact the Stable Time Increment of explicit solvers, as is the case with CEL. In weighing up these two factors, a suitably fine mesh is necessary to inhibit leakage but also yield results in a computationally efficient manner. Fig. 12 presents the q_c profile for various element sizes (side lengths in metres) at depths of 18–21 m. It is evident that convergence is obtained for the smallest two element sizes considered, while significant noise is noted for larger elements, which can be attributed to Eulerian leakage. A similar mesh sensitivity study is performed for all models herein, with the appropriate converged mesh results presented for brevity.

4. Spudcan penetration

Based on observations given by Overy (2012), recorded leg penetrations for each spudcan type at full leg preload were 3, 3.5–3.8, and 8 m for MLT 116-C, BREIT D-211 and Transocean 4, respectively. In the same study, four additional sites were considered, each with similar site conditions. These four additional locations (sites D – E) exhibited a very soft clay layer, separating the sand layers. Following CPT simulation, three different spudcan large deformation CEL models were created. Spudcan geometries for the MLT 116-C, BREIT D-221 and Transocean 4, in addition to model geometries and meshed parts are given in Figs. 13–15, respectively. In the case of MLT 116-C and Transocean 4, geometric symmetries allow for the use of a 45-degree wedge, rather than the full

360-degree geometry. Conversely, BREIT D-221 is unsuitable for axisymmetric analysis, instead requiring a full three-dimensional model setup. As a comparison of the requisite element distributions, the MLT, BREIT and Transocean models is given in Table 2. In the case of the BREIT and Transocean spudcan geometries, a significantly fine mesh was required to avoid penetration of Eulerian elements into the Lagrangian domain, as can be the case with coarsely meshed structures, or geometries involving considerable complexities with respect to the resolution of the Eulerian domain. Fig. 16 provides CEL model geometries for each of the 3 relevant soil domains. Although the Transocean 4 spudcan is significantly smaller than the two remaining spudcans, a fine mesh is required due to the complexity associated with the curvature of the geometry, involving a hollow section at the base of the spudcan. In the absence of penetration rate data for each of the spudcan cases, simulations for spudcan penetration were performed at a slightly higher penetration rate of 35 mm/s for the purpose of reducing simulation time costs. In each case, an associated 20 mm/s test case was performed to assure consistency with slower penetration rates. The soil sub-layers used in the aforementioned CPT simulations, in addition to their relevant soil parameters are preserved for each of the three spudcan models under consideration. Stress profiles at the commencement of penetration are given for each model, as shown in Fig. 17, while a comparison between simulated CEL load-penetration curves and field data given by Overy (2012) for each of the three rig geometries under consideration is detailed in Fig. 18. Considerable variation in the bearing capacities of the rigs is evident due to the shapes and sizes of each spudcan, in addition to the resultant stress distributions. The consistency of field test results compared with back-analysed CPT models
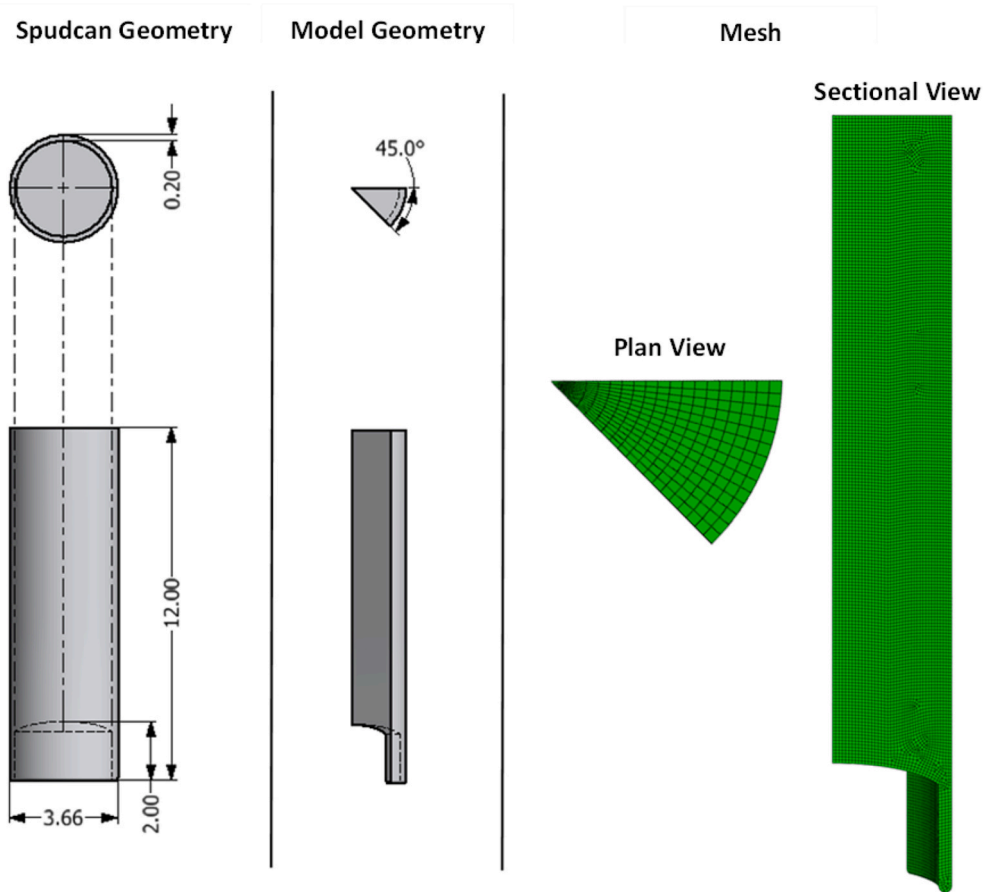
Fig. 14. Transocean 4 spudcan geometry and mesh distribution.

Spudcan: BREIT D-221
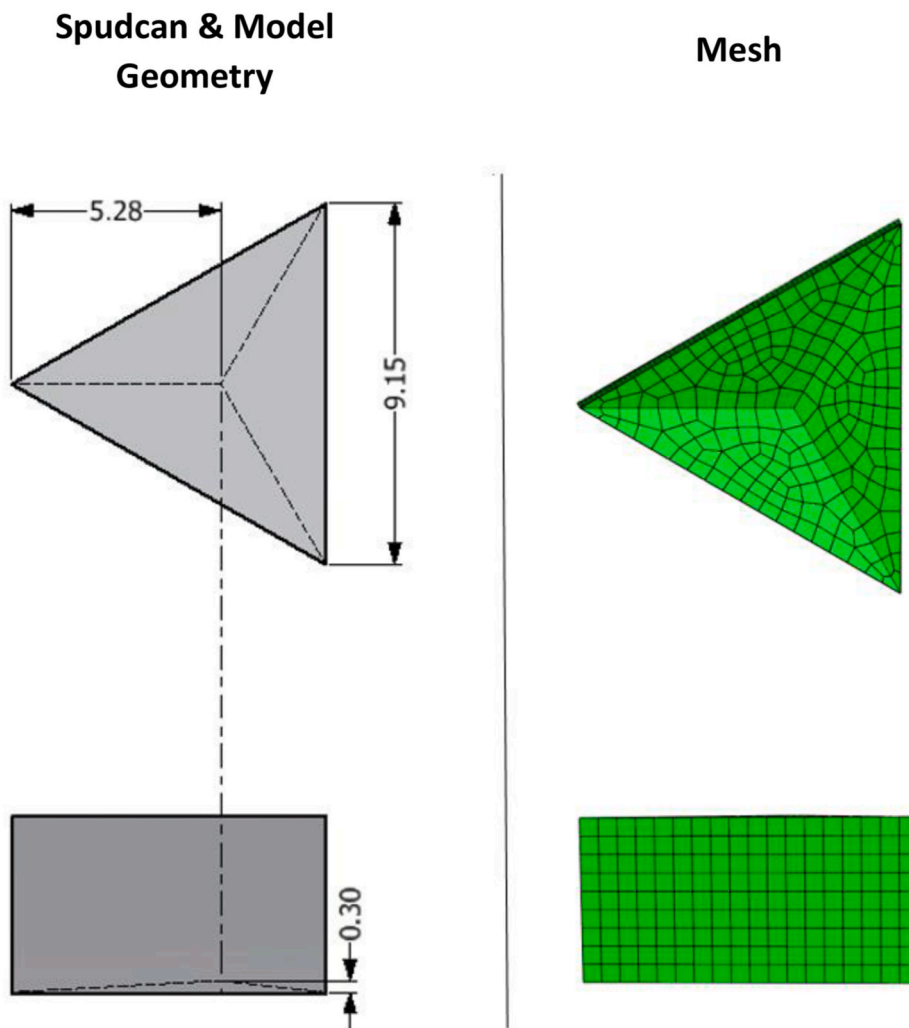
Spudcan & Model Geometry

Mesh

Fig. 15. BREIT D-221 spudcan geometry and mesh distribution.

Table 2
Spudcan model details.

Spudcan	Lagrangian Elements	Total Elements	Model type
MLT 116-C	586	21600	45-degree wedge
BREIT D-221	25389	267520	45-degree wedge
Transocean 4	11784	218376	360-degree geometry

used to develop and calibrate spudcan penetration models, highlights the practicality of the proposed method when combined with a procedure for assuming relevant soil properties in the presence of sparsely available geotechnical data.

5. Discussion and conclusion

The Coupled Eulerian Lagrangian method is a popular numerical technique for simulating the penetration of foundation structures into the seabed. In the case of the assessment of spudcan bearing capacities, often limited geotechnical test data are available, both from field and laboratory tests. As a result, significant risks to offshore foundations, such as punch through failure can be reliant on minimal or inaccurate observation data. A mechanism for back-analysing the behaviour of CPT field tests is presented, leveraging a procedure for obtaining the necessary soil characteristics for large deformation CEL simulation which allows for a variety of spudcan geometries to be assessed based without prior assumptions regarding failure mechanisms, as opposed to conventional standards such as SNAME and API, which are based on conventional bearing capacity theory for traditional spudcan geometries. The method is based on several well-known correlations of the relative density, peak friction angle and dilation friction angle of loose to medium-density sands. Back-analysis of soil stiffness parameters for thin sub-layers allows for soil characterisations suitable for CEL simulation of spudcan geometries. Through the use of a case study of a North Sea site, CEL spudcan load-penetration profiles are compared with field test data, providing strong agreement. While spudcan penetration is considered in where minimal field test data is presented, the method purposefully leverages CPT data to ensure that relevant numerical parameters are considered, with derived load penetration curves are consistent with the predictive method given by Overy (2012). As such, the method combining soil correlations and large deformation CPT back-analysis provides a convenient method for accurately determining the bearing capacity of spudcans involving unconventional geometries.
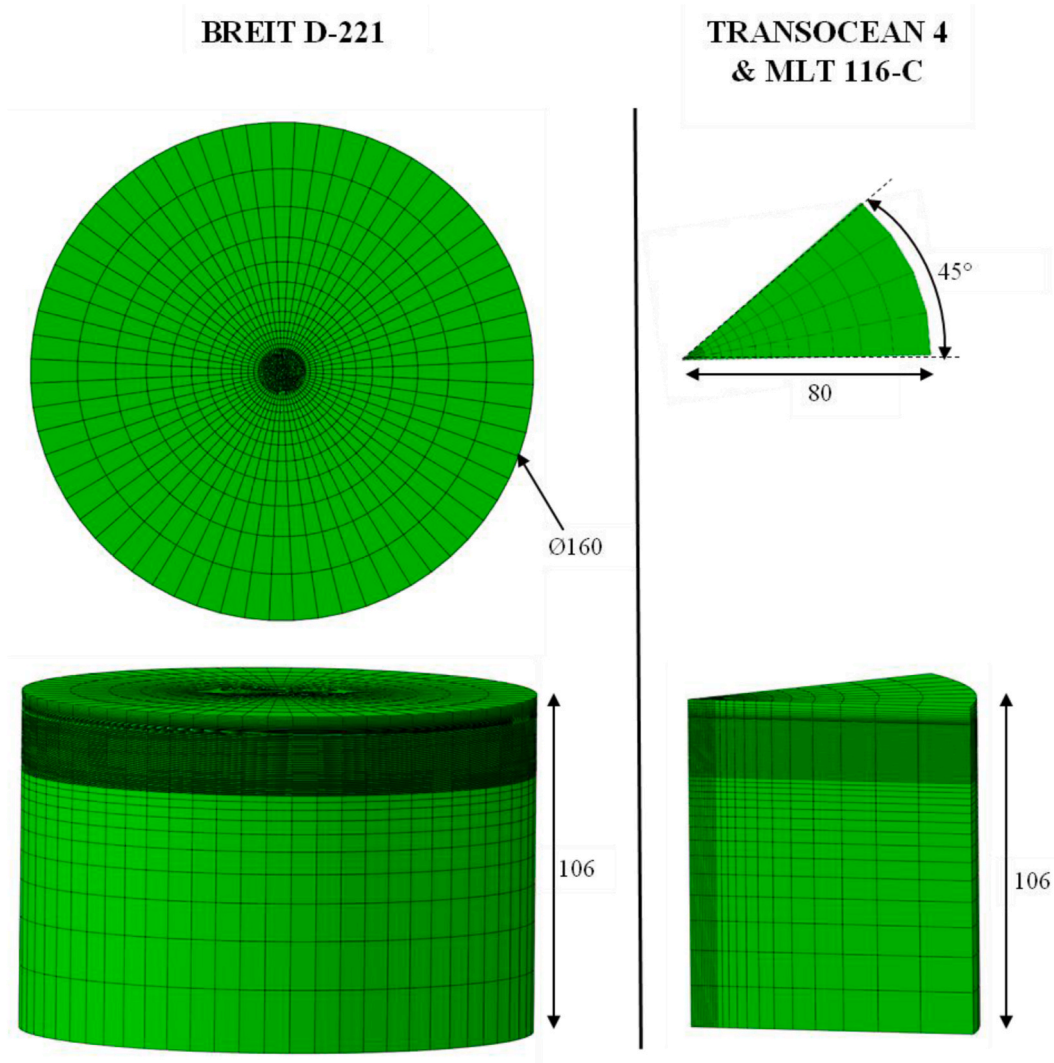
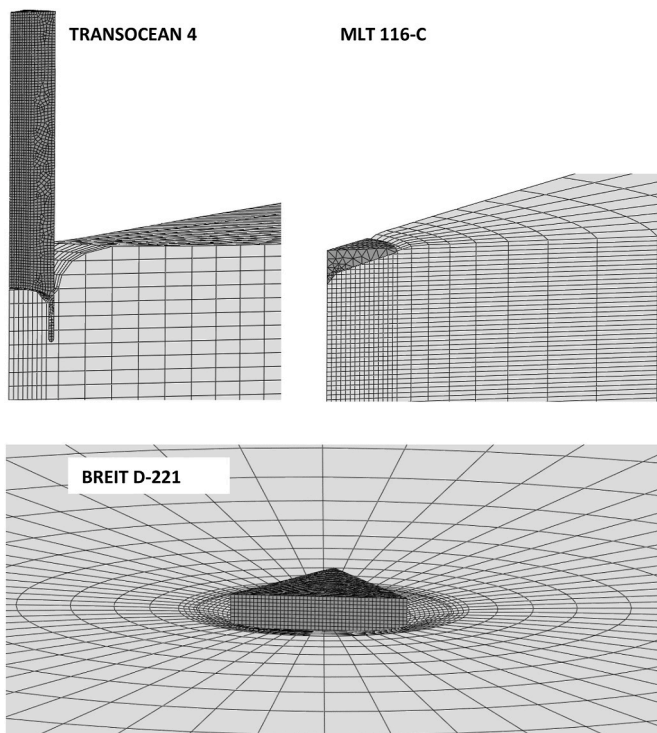**Fig. 16.** Soil geometries for CEL spudcan models and mesh distribution.

Fig. 17. CEL penetration into the soil domain for Transocean, MLT and Breit spudcans.
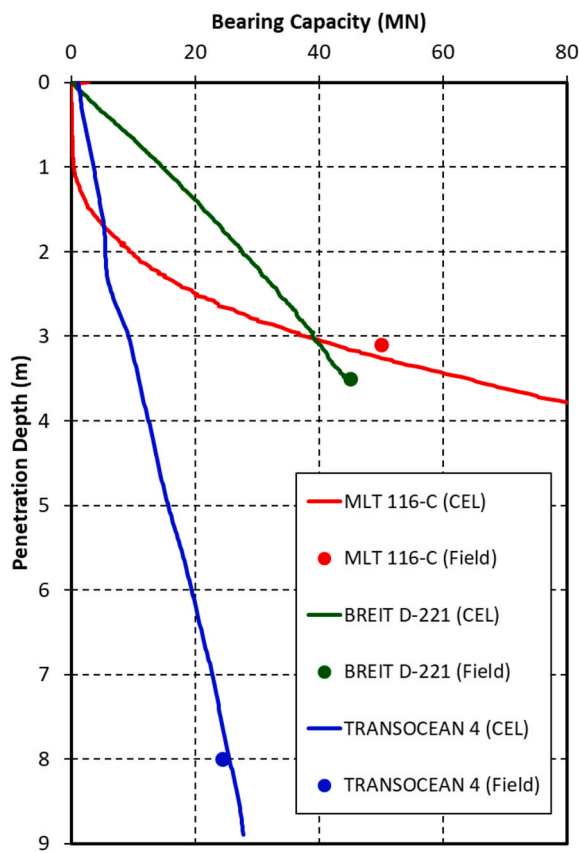

Fig. 18. Comparison between spudcan field test results and predictions using CEL.

Availability of data and material

Specific data can be provided on request by the corresponding author.

CRediT authorship contribution statement

Ali Tolooiyan: Data curation, Formal analysis, Investigation, Methodology, Validation, Visualization, Writing – original draft. **Kenneth Gavin:** Funding acquisition, Project administration, Supervision. **Ashley P. Dyson:** Conceptualization, Investigation, Visualization, Writing – review & editing.

Declaration of competing interest

The authors declare that they have no known competing financial interests or personal relationships that could have appeared to influence the work reported in this paper.

Data availability

Data will be made available on request.

Appendix A. Supplementary data

Supplementary data to this article can be found online at https://doi.org/10.1016/j.oceaneng.2024.117563.

References

Bienen, B., Henke, S., Pucker, T., 2011. Numerical study of the bearing behaviour of circular footings penetrating into sand. In: Proceedings of the 13th International Conference of the International Association for Computer Methods and Advances in Geomechanics (IACMAG).

Bolton, M., 1987. Discussion: the strength and dilatancy of sands. Geotechnique 37 (2), 219–226.

Campanella, R., Howie, J., 2005. Guidelines for the Use, Interpretation and Application of Seismic Piezocone Test Data. The University of British Columbia, Vancouver, Canada.

Ceccato, F., Beuth, L., Vermeer, P.A., Simonini, P., 2016. Two-phase material point method applied to the study of cone penetration. Comput. Geotech. 80, 440–452.

Chen, W.-F., Saleeb, A.F., 2013. Constitutive Equations for Engineering Materials: Elasticity and Modeling. Elsevier.

Chen, X., Zhang, L.L., Zhang, L., Yang, H., Liu, Z., Lacasse, S., Li, J., Cao, Z., 2020. Investigation of impact of submarine landslide on pipelines with large deformation analysis considering spatially varied soil. Ocean Eng. 216, 107684.

Dassault Systèmes, 2022. ABAQUS/Explicit 2022 [Computer software]. In).

Durgunoglu, H.T., Mitchell, J.K., 1973. Static Penetration Resistance of Soils.

Dutta, S., Hawlader, B., Phillips, R., 2012. Finite element modeling of vertical penetration of offshore pipelines using coupled Eulerian Lagrangian approach. In: The Twenty-Second International Offshore and Polar Engineering Conference.

Edwards, D., Bienen, B., Pucker, T., Henke, S., 2013. Evaluation of the performance of a CPT-based correlation to predict spudcan penetrations using field data. In: Proc. 14th Int. Conf. The Jack-Up Platform—Design, Design, Construction & Operation.

Gupta, T., Chakraborty, T., Abdel-Rahman, K., Achmus, M., 2016. Large deformation finite element analysis of static cone penetration test. Indian Geotech. J. 46 (2), 115–123.

Hamann, T., Qiu, G., Grabe, J., 2015. Application of a Coupled Eulerian–Lagrangian approach on pile installation problems under partially drained conditions. Comput. Geotech. 63, 279–290.

Henke, S., Qiu, G., 2010. Zum absetzvorgang von Offshore-hubplattformen. Geotechnik 33 (3), 284–292.

Holtz, R.D., 1991. Stress distribution and settlement of shallow foundations. In: Foundation Engineering Handbook. Springer, pp. 166–222.

Hossain, M., Randolph, M., 2010. Deep-penetrating spudcan foundations on layered clays: numerical analysis. Geotechnique 60 (3), 171–184.

Hu, P., Wang, D., Cassidy, M.J., Stanier, S.A., 2014. Predicting the resistance profile of a spudcan penetrating sand overlying clay. Can. Geotech. J. 51 (10), 1151–1164.

Hu, P., Wang, D., Stanier, S.A., Cassidy, M.J., 2015. Assessing the punch-through hazard of a spudcan on sand overlying clay. Geotechnique 65 (11), 883–896.

Huang, W., Sheng, D., Sloan, S., Yu, H., 2004. Finite element analysis of cone penetration in cohesionless soil. Comput. Geotech. 31 (7), 517–528.

ISO, 2012. Petroleum and Natural Gas Industries—site-specific Assessment of Mobile Offshore Units.

Jaly, J., 1944. The Coefficient of Earth Pressure at Rest. J. of the Society of Hungarian Architects and Engineers, pp. 355–358.

Jamiolkowski, M., Ladd, C., Germaine, J., Lancellotta, R., 1985. New developments in field and laboratory testing of soils. International conference on soil mechanics and foundation engineering 11.

Jamiolkowski, M., Lo Presti, D., Manassero, M., 2003. Evaluation of relative density and shear strength of sands from CPT and DMT. Soil behavior and soft ground construction 7 (119), 201–238.

Jun, M., Kim, Y., Hossain, M., Cassidy, M., Hu, Y., Sim, J., 2018. Numerical investigation of novel spudcan shapes for easing spudcan-footprint interactions. J. Geotech. Geoenviron. Eng. 144 (9), 04018055.

Lancellotta, R., 1983. Analisi di affidabilità in ingegneria geotecnica. Atti Istituto Scienza Costruzioni 625.

Lunne, T., Powell, J.J., Robertson, P.K., 2002. Cone Penetration Testing in Geotechnical Practice. CRC Press.

Mangiavacchi, A., Rodenbusch, G., Radford, A., Wisch, D., 2005. API offshore structure standards: RP 2A and much more. In: Offshore Technology Conference.

Martinelli, M., Galavi, V., 2021. Investigation of the material point method in the simulation of cone penetration tests in dry sand. Comput. Geotech. 130, 103923.

Mayne, P.W., Kulhawy, F.H., 1982. Ko- OCR relationships in soil. J. Soil Mech. Found Div. 108 (6), 851–872.

Nazem, M., Carter, J.P., Airey, D.W., 2009. Arbitrary Lagrangian–Eulerian method for dynamic analysis of geotechnical problems. Comput. Geotech. 36 (4), 549–557.

Osborne, J., Houlsby, G., Teh, K., Bienen, B., Cassidy, M., Randolph, M., Leung, C., 2009. Improved guidelines for the prediction of geotechnical performance of spudcan foundations during installation and removal of jack-up units. In: Proceedings of the 41st Offshore Technology Conference. OTC, Houston.

Overy, R., 2012. Predicting spudcan penetration in loose sand from measured site soil parameters. In: Offshore Site Investigation and Geotechnics: Integrated Technologies-Present and Future.

Qiu, G., Grabe, J., 2012. Numerical investigation of bearing capacity due to spudcan penetration in sand overlying clay. Can. Geotech. J. 49 (12), 1393–1407.

Randolph, M., Gourvenec, S., 2017. Offshore Geotechnical Engineering. CRC press.

Robertson, P.K., Campanella, R., 1983. Interpretation of cone penetration tests. Part I: sand. Can. Geotech. J. 20 (4), 718–733.

Rowe, P., 1971. Theoretical meaning and observed values of deformation parameters for soils. In: Proc. Of Roscoe Memorial Symposium, Cambridge Univ..

Schmertmann, J.H., 1970. Static cone to compute static settlement over sand. J. Soil Mech. Found Div. 96 (3), 1011–1043.

Schmertmann, J.H., 1978. Guidelines for Cone Penetration Test: Performance and Design.

SNAME, 2002. Guidelines for site specific assessment of mobile jack-up units. Soc. of Naval Arch. Mar. Eng. Tech. Res. Bull., 5-5A Rev. 2.

Tho, K.K., Leung, C.F., Chow, Y.K., Swaddiwudhipong, S., 2012. Eulerian finite-element technique for analysis of jack-up spudcan penetration. Int. J. GeoMech. 12 (1), 64–73.

Tian, Y., Cassidy, M.J., Randolph, M.F., Wang, D., Gaudin, C., 2014. A simple implementation of RITSS and its application in large deformation analysis. Comput. Geotech. 56, 160–167.

Tolooiyan, A., Gavin, K., 2011. Modelling the cone penetration test in sand using cavity expansion and arbitrary Lagrangian Eulerian finite element methods. Comput. Geotech. 38 (4), 482–490.

Tolooiyan, A., Gavin, K., Dyson, A.P., 2023. Estimation of spudcan penetration in variable sand deposits with the arbitrary Lagrangian eulerian finite element method. Ocean Eng. 281, 114955.

Zhang, S., Yi, J.T., 2018. Application of the Coupled Eulerian-Lagrangian finite element method on piezocone penetration test in clays. IOP Conf. Ser. Earth Environ. Sci. 153, 052054.

Zhang, T., Yi, J., Wang, Z., Liu, F., 2023. Numerical study on spudcan penetration-consolidation-uplift in soft soil using large deformation simulation. International Civil Engineering and Architecture Conference.